Research of Industrial Technology
Vol. 22, No. 1, 2004. 6

Journal of Applied Physics
Vol. 95, No. 10, May 2004

Optical and electrical properties of preferentially anisotropic single-walled carbon-nanotube films in terahertz region

Tae-In Jeon[a] and Keun-Ju Kim
Division of Electrical and Electronics Engineering, Korea Maritime University, Busan 606-791, Korea

Chul Kang, In Hee Maeng, and Joo-Hiuk Son
Department of Physics, University of Seoul, Seoul 130-743, Korea

Kay Hyeok An, Ji Yeong Lee, and Young Hee Lee
Department of Physics, National Research Laboratory for Carbon Nanotubes, Center for Nanotubes and Nanostructured Composites, Sungkyunkwan University, Suwon 440-746, Korea

(Received 14 October 2003; accepted 16 February 2004)

The absorption and dispersion of aligned single-walled carbon-nanotube films were measured from 0.2 to 2.0 THz using a source of freely propagating subpicosecond pulses of THz electromagnetic radiation. The real conductivity increased rapidly with increasing frequency up to 0.45 THz and decreased at a high-frequency range. The Maxwell–Garnett model, where the nanotubes were embedded in a dielectric host, fit the results of this study with the Drude–Lorentz model for nanotube network. We have observed the transverse phonon mode of 2.4 THz propagating along the *c* direction. This suggested that the carbon nanotube network is composed of metallic and semiconducting nanotubes embedded in an air dielectric host. © *2004 American Institute of Physics.* [DOI: 10.1063/1.1699498]

I. INTRODUCTION

The dynamic response of the electrical conductivity of single-walled carbon nanotubes (SWNTs) is an interesting subject from both fundamental and technological points of view. For instance, the frequency-dependent conductivity of SWNTs is directly related to the electromagnetic shielding in various electronic devices. The microwave and infrared properties of the SWNTs had been previously measured.[1,2] However, owing to the high THz absorption in carbon nanotubes, the dynamic response of carbon nanotubes for frequencies of several THz range is missing, and therefore is required for further comprehensive analysis of dynamic response in the far-infrared range.

The previous infrared absorption spectroscopy of SWNTs requires the Kramers–Kronig analysis over the frequency range of 15–5000 cm^{-1} (2–620 meV) to calculate the absorption and dispersion of the samples.[1] Recently, the dielectric properties of the SWNT films have been studied using electromagnetic waves up to 500 GHz.[2] The real conductivity was found to decrease with increasing frequency, in accordance with the Drude conduction model. However, in the far-infrared region, the spectrum showed a plasma edge with a Drude model combined with a low-frequency localized absorption.[1]

Another difficulty arises from the network of the crossed carbon nanotubes in the prepared SWNT thin film, which are composed of both metallic and semiconducting ones. Furthermore, these are sparsely embedded in air due to relatively low volume density, which makes the analysis more difficult. This has been modeled previously by the Maxwell–Garnet model, where the effective dielectric medium of multiwalled carbon nanotubes was composed of metallic and semiconducting (insulating) carbon nanotubes.[3] This model neglected the presence of empty (air) space created by the network of nanotubes in the film.

The characteristics of SWNTs were measured previously using terahertz time-domain spectroscopy (THz–TDS) until 0.8 THz.[4] We extended, in this approach, the range of dynamic responses of SWNTs up to 2.0 THz. The high-frequency range of our current measurement enabled us to be able to fit the phonon spectrum along the *c* direction. The simple Drude model could not explain this situation. Therefore, we introduced the Drude–Lorentz model combined with the Maxwell–Garnett (M–G) model. The M–G model, with a different interpretation from the previous work,[3] was introduced to fit the carbon nanotubes embedded in an effective dielectric air media with the Drude–Lorentz model to incorporate both metallic and semiconducting nanotubes. Our results showed that a significant portion of the conductivity was contributed from the localized states or phonon scattering from the doped semiconducting nanotubes, in contrast with previous reports of far-infrared response.

II. EXPERIMENT

SWNT powder was synthesized using a traditional arc discharge with catalytic transition metals.[5] The powder was a mixture of SWNTs and carbonaceous particles. It also contained a mixture of transition metals of about 15 wt % in the sample. To obtain a purified sample, this powder was heat treated at 470 °C for 30 min to remove carbonaceous particles. It was then refluxed in HNO_3 solution to remove transition metals.[5,6] The metal content was reduced to less than 1 wt %. This tar was mixed with 5 wt % binder (methylcellu-

[a]Electronic mail: jeon@mail.hhu.ac.kr

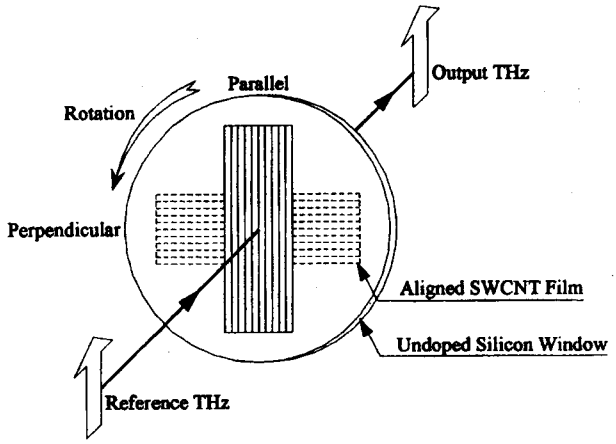

FIG. 1. Schematic diagram of aligned SWCNT film with polarized THz beam.

lose, which is water soluble) in distilled water, followed by sonication for 3 h. The thin film was obtained by mechanically squeezing the slurry on an undoped silicon window using a bar coater, which has almost no power absorption in the THz frequency range.[7] The film was 30 μm thick. Because of the uniaxial squeezing of the nanotube paste by the bar coater during film formation, substantial carbon nanotubes are aligned preferentially parallel to the squeezing direction. The anisotropy in the dc resistivity was measured to be nearly six over the wide range of temperatures.[8] This sample was placed into the THz–TDS system. The sample was then rotated parallel and perpendicular with respect to the beam polarization as shown in Fig. 1.

THz–TDS is based on the optoelectronic generation and reception of a beam of subpicosecond THz pulses. High-performance optoelectronic source was used to generate and detect the short pulses of THz radiation.[7,9] A GaAs transmission antenna and a silicon on sapphire receiving antenna were both optoelectrically driven by an average power of 10 mW from a mode-locked Ti:Sapphire laser. To eliminate the effects of water vapor on the THz beam,[7] the THz system was placed in an airtight dry box. Reference (without SWNTs) and output (with SWNTs) electromagnetic pulses were measured using the THz–TDS technique [Figs. 2(a) and 2(b)]. The shape of the output (transmitted) pulse was modified as it passed through the sample. Figure 2(c) shows the spectra of the measured THz pulses of the reference and the output with the sample placed parallel and perpendicular to the beam polarization.

The frequency-dependent absorption and dispersion of the sample were obtained using the Fourier analysis of the input and output pulses without using the Kramers–Kronig relationship. The imaginary index n_i was determined by the power absorption coefficient $\alpha = n_i 4\pi/\lambda$, where λ is the free-space wavelength. The real index n_r was obtained by the phase difference between the input and output pulses.

The filled and open circles in Figs. 3(a) and 3(b) show the measured power absorption and real index of refraction as a function of frequency. As can be observed in Figs. 3(a) and 3(b), the power absorption increases with increasing frequency, whereas the index of refraction decreases with frequency and saturates at high frequency. The index of refraction approached to about 1.8, corresponding to a real part of effective SWNT's dielectric constant $\epsilon_{\text{eff}}^{\infty}$ of 1.8^2. This value was smaller than 8.5 from the far-infrared measurement.[1] This was partly attributed to the existence of the nanotube network in the SWNT thin film, where the SWNT film was filled with air. Therefore, the observed dielectric constant is expected to be density dependent. The density of the nanotube film usually ranged from 0.5 to 1.0 g/cm^3, and is smaller than 1.63 g/cm^3 of graphite. It was difficult to measure the apparent density of the film used in this study, but it could be roughly estimated to range in the lower bound of the reported values.[1]

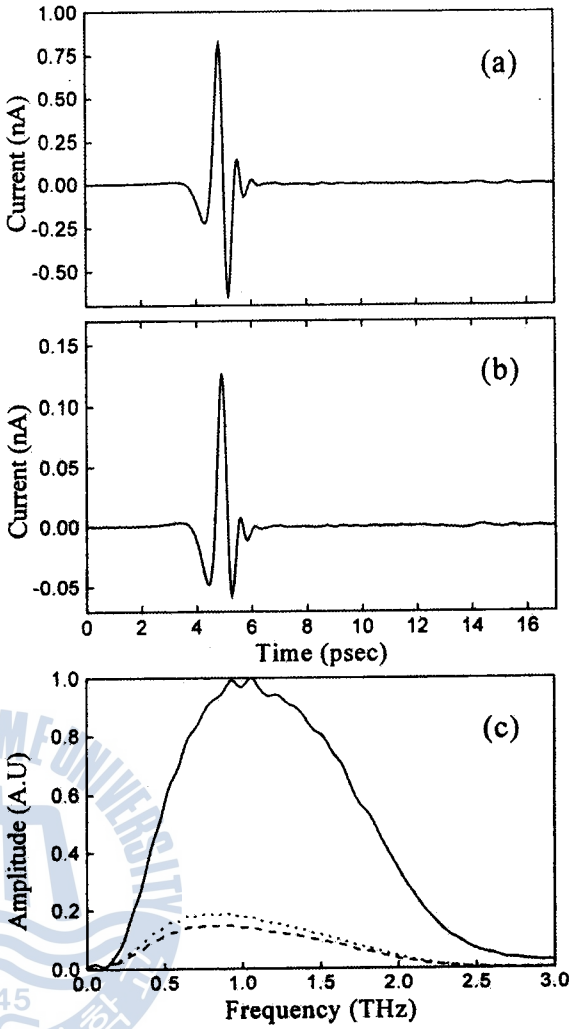

FIG. 2. (a) The reference THz pulse; (b) the THz pulse with the sample orientation parallel to the beam polarization; and (c) the amplitude spectra of the reference (solid line) and the sample orientation perpendicular (dotted line) and parallel (dashed line) to the beam polarization.

The effective dielectric response for a SWNT is described by the following general relationship:

$$\epsilon_{\text{eff}} = \epsilon_{\text{eff}}^{\infty} + i\sigma/(\omega\epsilon_0) = (n_r + in_i)^2. \quad (1)$$

dCollection

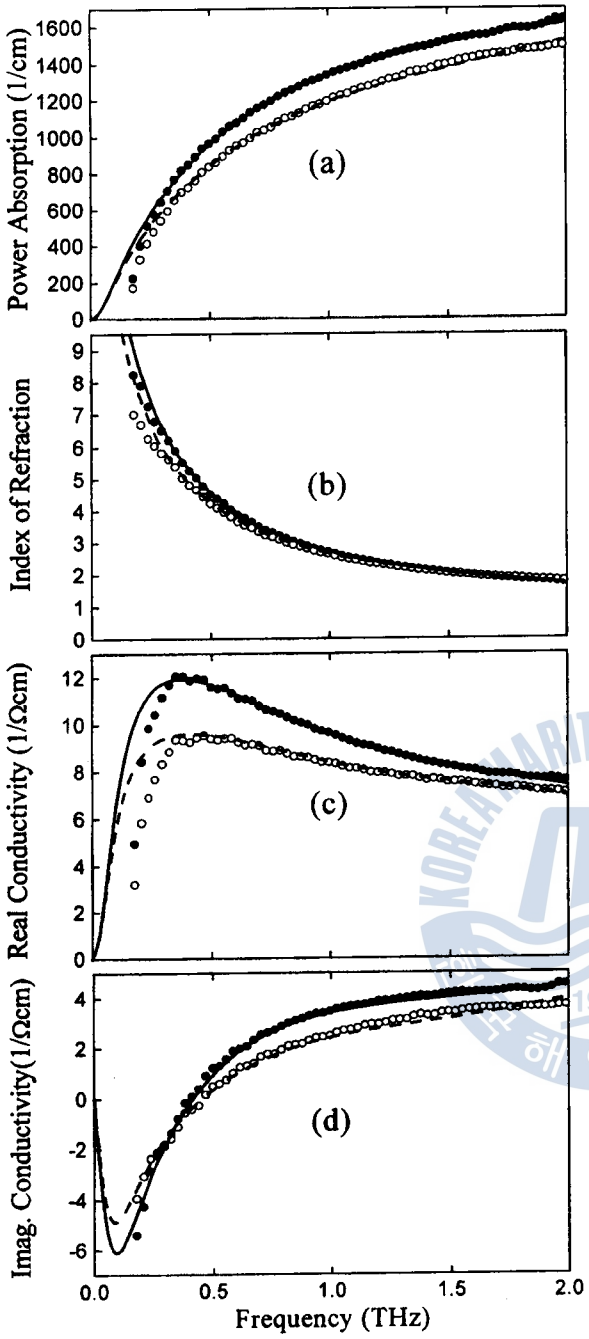

FIG. 3. Comparison of measurements (dots: Parallel and circles: Perpendicular) with theoretical model (solid line: Parallel and dashed line: Perpendicular), (a) power coefficient, (b) index of refraction, (c) real part conductivity, and (d) imaginary part conductivity.

The real conductivity could be obtained from $\sigma_{\text{Real}} = 2\omega\epsilon_0 n_r n_i$ and the imaginary conductivity from $\sigma_{\text{Imag}} = \omega\epsilon_0[\epsilon_{\text{eff}}^{\infty} - (n_r^2 - n_i^2)]$, where ϵ_0 is the free-space permittivity, as shown in Figs. 3(c) and 3(d). It is interesting to see that the real conductivity increased up to 0.45 THz at the low-frequency region, whereas the imaginary part gave negative values at the low-frequency region. We note that this peak frequency is slightly lower than the previous value of 0.65 THz.[4] This discrepancy was rather small, which could

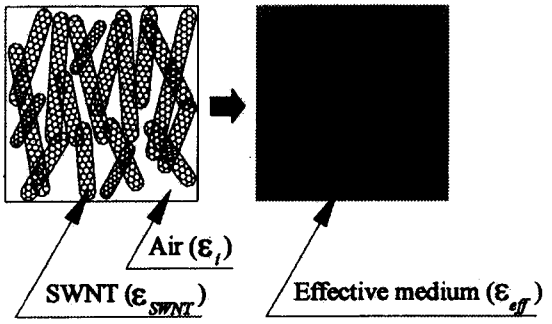

FIG. 4. SWNTs with dielectric constant (ϵ_{SWNT}) embedded by an insulator (ϵ_i) (left-hand side). The mixture results in an effective medium (ϵ_{eff}) (right-hand side).

be attributed to the different densities of samples with different batches. The previous sample, however, could not clearly show the resonance frequency due to the short terahertz range within 0.8 THz. In the current work, this resonance frequency was clearly seen with extended terahertz frequencies up to 2 THz. This suggests that the conductivity does not follow a simple Drude model in this frequency range. Instead, it requires a detailed analysis to explain such a complex behavior. It is also interesting to note that the conductivity anisotropy is about 1.4, at best near 0.45 THz, which is much smaller than that of dc resistivity anisotropy.[8] We speculate that this is probably due to the enhanced hopping by electromagnetic induction between the carbon nanotube network in the dynamic responses. The hopping rate could be dependent on the density of the film.

III. DISCUSSION

Figure 4 shows the effective medium with a carbon nanotube network embedded in an air medium. What we measured is the frequency-dependent effective complex dielectric constant ϵ_{eff}. To explain the dynamic response of such a medium, the M–G model was introduced, which is given by[3]

$$\epsilon_{\text{eff}} = \epsilon_i \frac{\{N + f(1-N)\}\epsilon_m + (1-N)(1-f)\epsilon_i}{N(1-f)\epsilon_m + (fN + 1 - N)\epsilon_i}, \qquad (2)$$

where f and N are the filling factor and geometrical factor of the M–G model, respectively. ϵ_m is the dielectric constant of the SWNT network which may be composed of metallic and semiconducting carbon nanotubes, and ϵ_i is the background dielectric constant to SWNTs. We should emphasize that our interpretation of the M–G model is quite different from the previous report, where ϵ_m and ϵ_i were interpreted as the dielectric constants of metallic and semiconducting nanotubes, respectively. We assumed in our approach that $\epsilon_i = 1$ because the SWNT network was filled with air. The geometrical factor N depended on the direction of the SWNT to the THz beam. When $f = 1$, only SWNTs were present in the film. When $f = 0$, no SWNT was present. In this study, we adopted $f = 0.9$, which was used for aligned cylinders of SWNTs.[3] f values of lower than 0.9 could not fit the measured curve. The fitted geometrical factors (Table I) were almost independent of the aligned direction of the SWNTs

Collection

TABLE I. Theoretical fitting parameters for the measurements presented in Figs. 1(a)–1(d).

Parameter	$\omega_p/2\pi$ (THz)	$\Gamma/2\pi$ (THz)	$\omega_{pj}/2\pi$ (THz)	$\omega_j/2\pi$ (THz)	$\Gamma_j/2\pi$ (THz)	N
Parallel	5.40	1.17	6.19	2.40	4.56	0.040
	±0.5	±0.25	±0.8	±0.22	±0.5	±0.003
Perpendicular	5.65	1.60	4.32	2.32	2.96	0.046
	±0.35	±0.22	±0.36	±0.18	±0.15	±0.003

within the fitting error. Therefore, the alignment of SWNTs did not appreciably affect the effective dielectric constant.

We next considered ϵ_m as a network of both metallic and semiconducting nanotubes that forms cross junctions between metallic and semiconducting nanotubes.[8,10] This could be modeled by a combination of the Drude term and localized Lorentzian absorption, given by[1]

$$\epsilon_m(\omega)=\epsilon^{\infty}_{\mathrm{SWNT}}-\frac{\omega_p^2}{\omega^2+i\Gamma\omega}+\sum_j\frac{\omega_{p,j}^2}{(\omega_j^2-\omega^2)-i\Gamma_j\omega}, \quad (3)$$

where ϵ^{∞}_{SWNT} is the dielectric constant of the SWNT network. The dielectric constant of an effective medium at infinite frequency $\epsilon_m(\infty)\approx 1.87^2$ could be calculated using $\epsilon^{\infty}_{\mathrm{eff}}=1.8^2$, $\epsilon_i=1$, $N=0.040$ (0.046 for perpendicular), and $f=0.9$ in Eq. (2), which can be used for $\epsilon^{\infty}_{\mathrm{SWNT}}$ in Eq. (3). ω_p is the plasma frequency, Γ is the damping rate, ω_j is the phonon frequency, Γ_j is the spectral width, and ω_{pj} is the oscillator strength of the Lorentz oscillators. The first and second terms are well known as a Drude model for a good metal. In the simple Drude model, the key parameters describing the dynamics of free carriers in a material are ω_p and $\Gamma=1/\tau$, where τ is the carrier collision time. The third is a Lorentz oscillator term by phonon mode. Only a single Lorentzian oscillation was needed to obtain a good fitting with the measurements in our study.

Figure 5 shows the relationship between the M–G model combined with Lorentz–Drude model, the Drude model, and the Lorentz oscillator for the perpendicular component until 2 THz. The Drude model corresponded to the first and second terms in Eq. (3), while the Lorentz oscillator curve was represented by the third term. The M–G model was plotted by combining Eqs. (2) and (3). Because the Lorentz oscillator had a very small real conductivity at a low-frequency range, the conductivity of the M–G model decreased with decreasing frequency, as shown in Fig. 5(c). The imaginary conductivity of the M–G model also became negative at low frequencies due to the presence of small imaginary conductivity in the Lorentz oscillator. We emphasize that the decrease in the conductivity is realistic, since the power loss occurs near 0.2 THz, as indicated in Fig. 2(c). Figure 3 shows the fitted curves (denoted by solid lines) using the M–G model to the measured ones based on the parameters in Table I. In spite of several fitting parameters, very reliable parameter sets with a relatively lower range of fitting errors were found.

Characteristically, several parameters had the range of THz frequencies. The plasma frequency ω_p is 5.4 THz and 5.65 THz for parallel and perpendicular, respectively. This

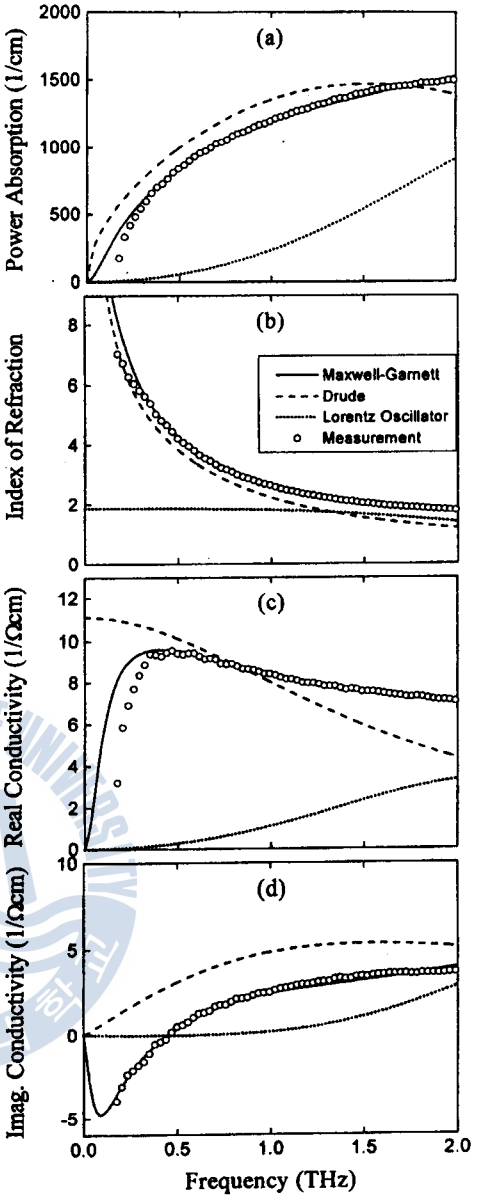

FIG. 5. Comparison of various theories and perpendicular measurement (solid line: M–G model using Drude term and Lorentz oscillator, dashed line: Drude model, dotted line: Lorentz oscillator, and circles: Measurement), (a) power absorption, (b) index of refraction, (c) real part conductivity, and (d) imaginary part conductivity.

value is similar to that obtained from the Drude model up to 0.5 THz.[2] However, it is significantly smaller than the previously reported one, which was obtained from the Drude–Lorentz model with frequency ranges from 0.5 THz to infrared region.[1] This discrepancy is not clear at this moment. The fitted damping rate was $\Gamma/2\pi=1.17$ and 1.60 THz for the parallel and perpendicular components, respectively, corresponding to the collision times of $\tau=136$ and 99 fs. This was closely related to the effective scattering length of nanotubes. Since nanotubes could be regarded as a mat formed by cross junctions, and thus the parallel component has longer nanotubes between junctions,[8] one may imagine that nanotubes do not act as a scattering center but the cross junctions are

dCollection

responsible for determining the collision time. The collision length could be estimated at $\ell = \nu_F \tau \sim \mu$m, an order of nanotube length, where ν_F is the Fermi velocity of nanotubes, supporting our assertion. The M–G model has been also introduced to fit the measured conductivity in the terahertz region.[11] Since the available data were only up to 0.8 THz with a resonance frequency at 0.65 THz, the resonance was not fully incorporated, giving a different set of fitting values. Here, since we extended the frequency up to 2 THz, the resonance was fully encountered during the fitting and therefore more reliable fitting parameters were obtained.

The power absorption coefficient of the parallel and perpendicular samples showed a consistent increase with increasing frequency [Fig. 3(a)]. Because of the frequency response of the THz–TDS system, the measured data were reliable only above 0.2 THz. The power absorption of the parallel orientation was always larger than that of the perpendicular orientation because of higher conductance due to longer effective length of carbon nanotubes compared with the perpendicular orientation.[8] The measured results were well fit with the M–G model combined with Drude–Lorentz model. Although the results shown in Figs. 3(a) and 3(b) could be related by Kramers–Kronig relationship, they were measured independently in this study. However, the deviations were very small in the high-frequency range. The measured real part of the conductivity increased with increasing frequency and did not follow the simple Drude behavior[12] which has a Lorentzian line shape centered at zero frequency.[13,14] As described above, the measurements in this study were well fitted with the M–G model [Fig. 3(c)]. The measured real conductivity became lower than the theoretical M–G model in Fig. 3(c) only at lower frequencies. Because of the deficiency of the THz beam power below 0.2 THz, the agreement between measurements and the M–G model could not be ensured. The real conductivity from the M–G model at a high-frequency range was higher than that from the fitting of the simple Drude model, as shown in Fig. 5(c). This discrepancy is related to the phonon absorption along the c direction with a center frequency of 2.40 THz. This phonon absorption is similar to the previous reports.[1,3,15] We conclude that our measured conductivity at the high-frequency region involves contributions from both phonon responses and electron responses.

The measured imaginary conductivity in Fig. 3(d) showed a strong frequency dependence, where at low-frequency region, the M–G model gave a well-resolved minimum with negative values, although the measured values were not obtained below 0.2 THz due to the limited THz beam power. The imaginary conductivity was negative until 0.45 THz, the same frequency of maximum power absorption. This is closely related to the proximate zero region in the Lorentzian model, which is shown in Fig. 5(d). The M–G model surely overweighs this region, giving rise to the negative values in the imaginary conductivity.

IV. SUMMARY

We have measured absorption and dispersion of the aligned SWNT film from 0.2 to 2.0 THz without invoking the Kramers–Kronig relationship. The real conductivity increased with increasing frequencies that did not follow the simple Drude model at a low-frequency range. By employing the M–G model combined with the Drude–Lorentz model to explain the carbon nanotube network in an effective air medium, we have fitted the measured conductivity. In particular, at a high-frequency range, we were able to fit by considering both electron absorption and phonon absorption along the c direction.

ACKNOWLEDGMENTS

This work was supported by the Korea Research Foundation by Grant No. KRF-2000-015-DP0163. One of the authors (Y.H.L.) acknowledges financial support from MOST through NRL and the KOSEF through CNNC at SKKU.

[1] A. Ugawa, A. G. Rinzler, and D. B. Tanner, Phys. Rev. B **60**, R11305 (1999).
[2] O. Hilt, H. B. Brom, and M. Ahlskog, Phys. Rev. B **61**, R5129 (2000).
[3] K. Tanaka, T. Yamabe, and K. Fukui, *The Science and Technology of Carbon Nanotubes* (Elsevier, New York, 1999).
[4] T.-I. Jeon, K.-J. Kim, C. Kang, S.-J. Oh, J.-H. Son, K. H. An, D. J. Bae, and Y. H. Lee, Appl. Phys. Lett. **80**, 3403 (2002).
[5] Y. S. Park, K. S. Kim, H. J. Jeong, W. S. Kim, J. M. Moon, K. H. An, D. J. Bae, G. S. Park, and Y. H. Lee, Synth. Met. **126**, 245 (2002).
[6] J. M. Moon, Y. S. Park, K. H. An, G. S. Park, and Y. H. Lee, J. Phys. Chem. **105**, 5677 (2001).
[7] D. Grischkowcky, S. Keiding, M. van Exter, and C. Fattinger, J. Opt. Soc. Am. B **7**, 2006 (1990).
[8] D. J. Bae, K. S. Kim, Y. S. Park, E. K. Suh, K. H. An, J. M. Moon, S. C. Lim, S. H. Park, Y. H. Jeong, and Y. H. Lee, Phys. Rev. B **64**, 233401 (2001).
[9] J.-H. Son, T. B. Norris, and J. F. Whitaker, J. Opt. Soc. Am. B **11**, 2519 (1994).
[10] M. S. Fuhrer, J. Nygard, L. Shih, M. Forero, Y. G. Yoon, M. S. C. Mazzoni, H. J. Choi, J. Ihm, S. G. Louie, A. Zettl, and P. L. McEuen, Science **288**, 494 (2000).
[11] J. Han, Z. Zhu, Z. Wang, W. Zhang, L. Yu, L. Sun, T. Wang, F. He, and Y. Liao, Phys. Lett. A **310**, 457 (2003).
[12] T.-I. Jeon, D. Grischkowsky, A. K. Mukherjee, and R. Menon, Appl. Phys. Lett. **79**, 4142 (2001).
[13] T.-I. Jeon and D. Grischkowsky, Phys. Rev. Lett. **78**, 1106 (1997).
[14] T.-I. Jeon and D. Grischkowsky, Appl. Phys. Lett. **72**, 2259 (1998).
[15] R. Nicklow, N. Wakabayashi, and H. G. Smith, Phys. Rev. B **5**, 4951 (1972).

Collection